ORIGINAL PAPER

Experimental investigation of the interaction between water and shear-zone materials of a bedding landslide in the Three Gorges Reservoir Area, China

Xuan Kang[1] · Guangli Xu[1] · Zhang Yu[1,2] · Shun Wang[3] · Mengting Wang[1]

Abstract

Most landslides induced by reservoir impoundment and rainfall in the Three Gorges Reservoir area of China are usually characterized by bedding-plane shear zones. This paper presents an experimental study of the interaction between water and shear-zone materials. A series of tests, including wetting-drying cycles and soaking tests, were carried out. The results show that the fluid-solid interaction not only reduces the shear strength of shear-zone soil but also accelerates the disintegration process of clastic rock from shear zone. After the fluid-solid interaction at different pH values, the clastic rock samples produce the most clay minerals in acidic solution. Similarly, the clay minerals of shear-zone soil samples increase dramatically after 45 days of soaking in acidic environment. According to the tests, it is found that the shear-zone soil in eluvium may originate from the weathered clastic rock near the shear zones under long-term fluid-solid interaction.

Keywords Fluid-solid interaction · Shear-zone soil · Wetting-drying cycles · Clay minerals · Evolution relationship

Introduction

Landslides become the most common, catastrophic geohazard in the Three Gorges Reservoir (TGR) area of China after the first impoundment in 2003. Since the occurrence of the Qianjiangping landslide (Wang et al. 2004), researchers have realized that not only precipitation but also fluctuations of reservoir water level can affect the stability of landslides (Paronuzzi et al. 2013; Xia et al. 2015; Wang et al. 2018). The operation of TGR gives rise to 30-m water level fluctuations in the reservoir, with 175 m to 145 m to 175 m in each hydrological year. The slope soil above and below the 145-m elevation undergoes periodic wetting-drying and soaking

conditions, respectively. Moreover, the discharge of pollutants in the TGR area prevents the reservoir water from maintaining neutrality (Müller et al. 2008; Ye et al. 2011), and these pollutants may have side effects on the soaked slope bank. The interaction between fluid and slope soil combined with external hydraulic conditions, such as reservoir water fluctuation and seasonal rainfall, may lead to potential failure in the slopes (Iverson 2000; Baum et al. 2010; Lora et al. 2016; Wang et al. 2020).

In nature, it is believed that the fluid-solid interaction plays a key role in the generation of landslides in the range of decades or hundreds of years. To mimic this geological process in the laboratory, some well-designed tests, such as wetting-drying cycles and specific chemical treatments, can be adopted to accelerate the process of fluid-solid interactions. Previous researches have revealed that wetting-drying cycles will give rise to weakening effects on the physical and mechanical properties of geomaterials (Calvello et al. 2005; Aldaood et al. 2014; Özbek 2014). Usually, the slope soil would experience a remarkable reduction in shear strength after the wetting-drying cycles, and in particular, the weak layers in slopes will be significantly affected (Dif and Bluemel 1991; Kanyaya and Trenhaile 2005; Tang et al. 2011). On the other hand, the chemical changes of the pore fluid, e.g. composition and concentration, will also largely

✉ Guangli Xu
xu1963@cug.edu.cn

[1] Engineering Faculty, China University of Geosciences, Wuhan 430074, People's Republic of China

[2] Central Southern China Electric Power Design Institute Co, LTD. of China Power Engineering Consulting Group, Wuhan 430063, People's Republic of China

[3] Institut für Geotechnik, Universität für Bodenkultur, Feistmantelstrasse 4, A-1180 Vienna, Austria

affect the shear behaviour and internal minerals of soil (Mesri and Olson 1970; Di Maio et al. 2004, 2015).

A close inspection of the relevant literature reveals, however, that most studies focus either on the wetting-drying effect or the chemical treatment effect on slope soil (Bjerrum and Rosenqvist 1956; Sridharan and Prakash 1999; McKissock et al. 2002; Majdalani et al. 2008), while few studies have compared their difference in these effects. Particularly, there are no detail discussions on the rock-soil transformation in the shear zone of landslides. In this paper, we study the interaction between water and the shear-zone materials taken from a bedding landslide in the TGR area. A series of wetting-drying cycle tests and soaking tests with solutions at different pHs are performed. Some reversal direct shear tests are supplementarily carried out to investigate the effects of fluid-solid interaction on the shear strength of the shear-zone soil samples. In addition, the grain size distribution of the clastic rock samples in shear zones is also analysed during the tests. Based on the experimental results, the rock-soil transformation mechanism in the shear zone is discussed.

Characteristics of the Shanshucao landslide

The Shanshucao landslide occurred on September 2, 2014. It is located on the left bank of the Luogudong River, a secondary tributary of the Yangtze River in Shazhenxi Town, Zigui County, Hubei Province. The landslide is only 0.75 km from the well-known impoundment-induced landslide, the Qianjiangping landslide, and approximately 42 km from the Three Gorges Dam (Fig. 1). The average slope of the Shanshucao landslide varies from 18 to 25°, and the altitude of the bedrock layer varies from 120 to 125°∠19–21°. The landslide had an average width of 130 m in the north-south direction and an average length of 300 m in the west-east direction. The landslide varies from 140 to 283 m a.s.l., and below 175 m a.s.l. the sliding mass was affected by the reservoir water-level fluctuations. Before the occurrence of the landslide, a small hydropower station (180 m a.s.l.) and a national highway G348 (204 m a.s.l.) located on the sliding area. An approximately 55×10^4 m^3 sliding mass poured into the Luogudong River at a high speed with a runout distance of 160 m, leading to a total landslide area of 3.8×10^4 m^2. The landslide destroyed the road G348 and instantly pushed the hydropower station into the Luogudong River, which had a water level of 162.3 m a.s.l. at that time.

The geological strata within the site are mainly composed of Quaternary sediments (Q$_4$) and Middle Jurassic Qianfoya formation (J$_{2q}$) (see Fig. 2). The former includes eluvium, collapse, and landslide deposits. They are a combination of silty clay with fragmented rock, observed commonly on the surface and sliding mass of the landslide, with the main

component of the fragmented rock being from J$_{2q}$. The latter is widely distributed in the sliding mass. According to the field survey after the landslide, the lithology of the sliding mass is identified as silty mudstone, argillaceous siltstone, and feldspar quartz sandstone, which are relatively fragmented. In addition, muddy interlayers, which contain rock debris, fine particles, and argillaceous products, with relatively thin thicknesses and intact surrounding rock layers, are commonly observed in the study area. A 5–15-cm thick shear zone is observed in a muddy interlayer between the bedrock and the sliding mass. This shear zone is believed to dominate the main movement of the landslide, and the main shear-zone soil is composed of grey-green silty clay with breccia. Additionally, there is a secondary shear zone accounts for the minor motion of the landslide and developed on the north boundary of the landslide. The shear-zone soil is silty clay in the eluvium with yellow colour. The bedrock is a complete J$_{2q}$ grey-green sandy shale with scratches on the surface. The thickness of the bedrock is approximately 23–30 m with an attitude of 120°∠20°.

It is well-known that the hydrological condition is significant for the occurrence of a landslide. As reported by Xu et al. (2015), the sudden movement of the Shanshucao landslide resulted from the accumulated rainfall and a rapid impoundment in the TGR. The groundwater in the site consists of pore water in the Q$_4$ deposit and fissure water in the J$_{2q}$ bedrock. To investigate the water characteristic of the landslide, some water samples were taken from different locations of the landslide (see Fig. 3). Table 1 shows the chemical composition of the water samples. The results reveal that the main ions of the water samples are HCO$_3^{3-}$, SO$_4^{2-}$, Ca$^+$, K$^+$, and Na$^+$; therefore, the water samples of the landslide exhibits neutral-alkalescence.

Shear-zone materials and testing procedure

Test materials and preparation

In order to study the effect of water on the shear-zone materials in the laboratory, some intact soil samples were taken from the two shear zones, which are exposed after the landslide. The locations of intact soil samples can be seen in Fig. 3. Two of these samples (samples S$_1$ and S$_2$, representing shear-zone soil in the muddy layer and eluvium, respectively) were used to determine their basic properties and grain size distributions.

Table 2 shows the general physical properties of the intact samples. The two soil samples can be described as silt-clay with low to medium plasticity, and soil sample in the muddy interlayer of the main shear zone (S$_1$) shows lower plasticity. The results of the grain-size analysis of the soil samples are shown in Fig. 4. For intact soil samples, the maximum particle
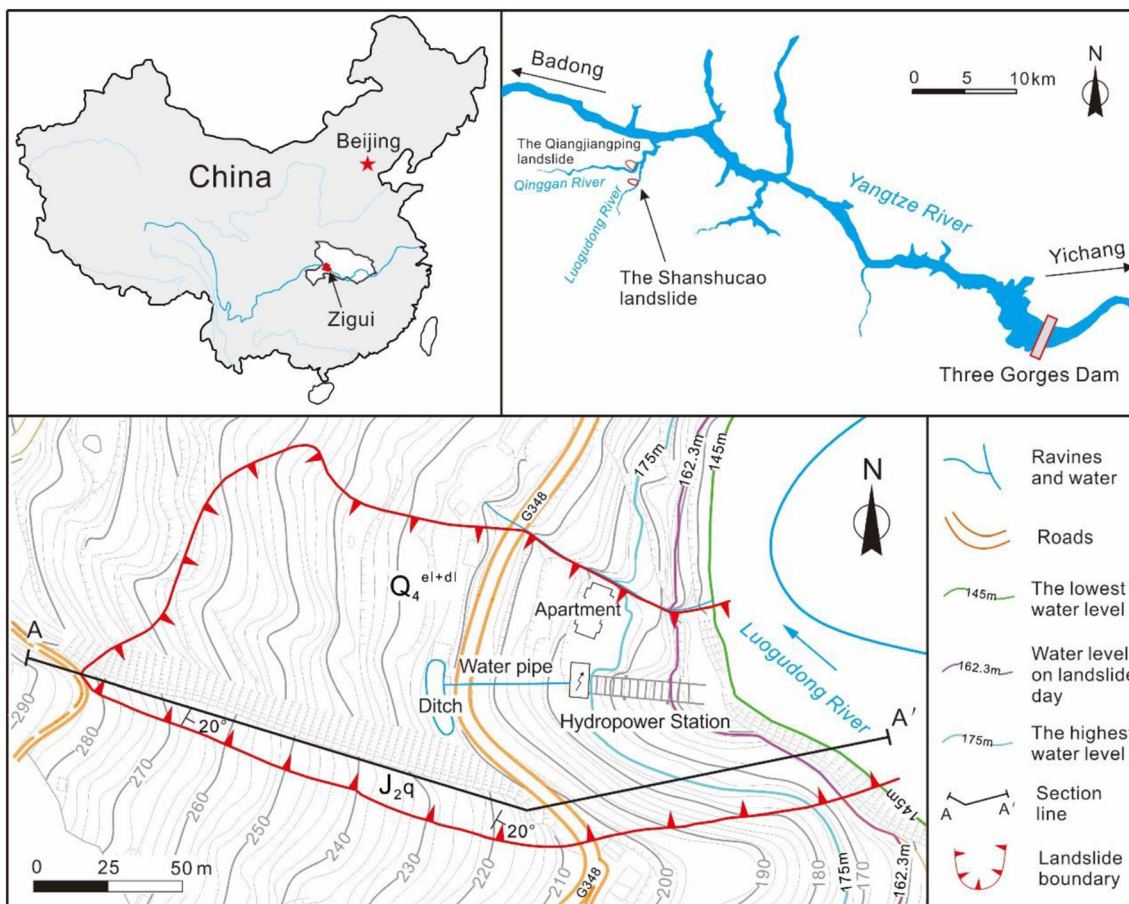
Fig. 1 Location and plan view of the Shanshucao landslides (modified after Xu et al. 2015)

diameters both exceed 5 mm. The sample S_2 has more coarse-grained particles (larger than 2.0 mm in diameter, denoted as $d > 2.0$ mm) with a percentage of 70%, while the sample S_1 contains more fine-graded particles. In addition, the fraction of finer particles ($d < 0.1$ mm) was determined by laser testing after the dispersion treatment using a Malvern UK Mastersizer 3000. As presented in Fig. 5a, the fine-grained particles (silt + clay) accounts for 97 and 67 wt.% in samples S_1 and S_2,

respectively. The grain frequency distribution curve is characterized by the concentration of finer particles, at approximately 4 μm for sample S_1, and 5 to 12 μm for sample S_2, at which the curves are multimodal (see Fig. 5b). The coefficients of uniformity (CU) are 9.13 and 11.67 for samples S_1 and S_2, respectively; hence, sample S_2 is well sorted and more uniform than sample S_1. The result implies that the composition of shear-zone soil developed in the muddy interlayer is

Fig. 2 Section A-A′: ① feldspar quartz sandstone; ② silty mudstone; ③ sandy shale; ④ muddy interlayer; ⑤ eluvium; ⑥ rock debris (modified after Xu et al. 2015)
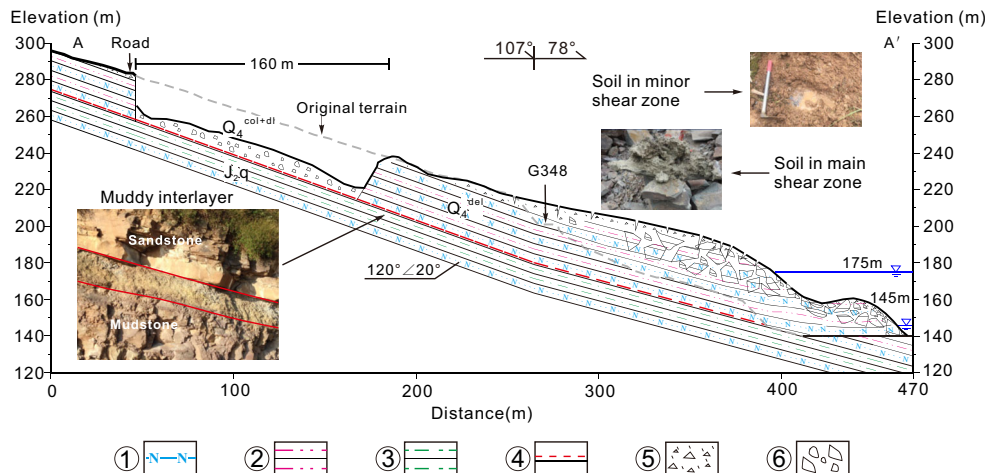
Fig. 3 Location of the test samples
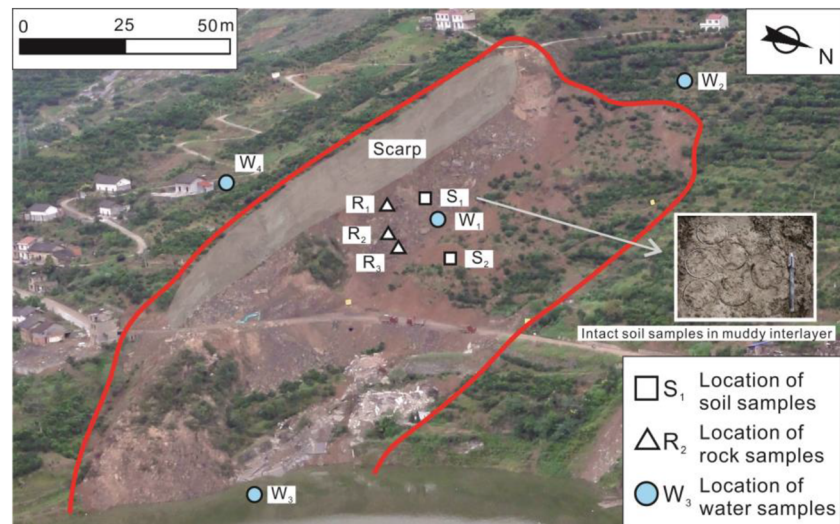
relatively homogeneous while the one developed in eluvium may be a mixture of various sediments with coarse-grained soil combined with fine particles.

Since the particles of the intact shear-zone soils are too large for subsequent laboratory test, remoulded soils with a particle size less 2 mm were used in the tests. The grain size distribution compared with intact samples is shown in Fig. 4. The proportion of particles larger than 0.075 mm in diameter ($d > 0.075$ mm) reached 23.2 wt.% in the sample S_1, while only 9.1 wt.% in the sample S_2. The two kind of soils were reconstituted with similar dry densities and water contents to those of the intact soils, i.e. dry density $\rho_d = 1.8$ g/cm^3 and 1.7 g/cm^3 for sample S_1 and S_2, respectively, and water contents $W = 16\%$ and 17% for sample S_1 and S_2, respectively. Then these prepared soils were made into specimens, which have a total volume of 59.9 cm^3 with a round area of approximately 30 mm^2 and height of 20 mm.

In addition to the shear-zone materials, we also investigated the internal structure of the bedrock below the shear zone by using a polarizing microscope with slice samples. Figure 6 indicates that the bedrock is consisted of mainly silty mudstone, argillaceous siltstone, and quartz sandstone, which contains quartz, feldspar, mica, and argillaceous minerals. The argillaceous content in the silty mudstone is nearly 43%, which is slightly higher than that of the argillaceous siltstone (30–33%), and the quartz content in quartz sandstone is close to 85%. It is evidenced by the photomicrographs that the mineral particles, such as quartz and feldspar, are bonded by shale cement. The argillaceous content in rock samples explain that the exposed surface of mudstone is usually weathered into debris while the sandstone layer is relatively intact.

To better understand the interaction between water and shear-zone materials, we also collected some clastic rock samples near the two shear zones (locations see Fig. 3). Three type of clastic rock samples with various initial size, namely R_1

Table 1 Characteristics and analysis of water samples

Samples		W_1	W_2	W_3	W_4
Content (mg/L)	Ca^{2+}	35.3	17.6	41.7	57.7
	Mg^{2+}	7.8	5.4	7.8	13.6
	$K^+ \cdot Na^+$	9.3	25.1	14.8	7.8
	Cl^-	4.2	6.2	10.5	18.0
	SO_4^{2-}	16.8	36.1	29.7	88.3
	HCO_3^-	140.3	61.0	146.5	119.6
	CO_3^{2-}	–	12.0	–	–
	Salinity	213.5	163.4	250.8	305.0
	Free CO_2	7.0	0.0	10.6	6.2
	Corrosive CO_2	0.0	0.0	0.0	0.0
pH		7.9	8.9	7.8	7.7
Main ions		HCO_3-Ca	$HCO_3 \cdot SO_4$-(K + Na)·Ca	HCO_3-Ca	$HCO_3 \cdot SO_4$-Ca

Free CO_2 is carbon dioxide that can be dissolved in water, and corrosive CO_2 is the excessive free CO_2 that is beyond the balance in water

Table 2 Basic properties of the shear-zone soil

Sample name	ρ (g/cm^3)	ρ_d (g/cm^3)	W (%)	W_L (%)	W_P (%)	I_P (%)
S$_1$ (soil in muddy interlayer)	2.0~2.3	1.7~1.9	15.9~18.3	29.7	16.3	13.4
S$_2$ (soil in eluvium)	1.9~2.0	1.7~1.8	17.0~18.8	33.6	18.3	15.3

ρ bulk density, ρ_d dry density, W water content, W_L liquid limit, W_P plastic limit, I_P plasticity index

(mudstone fragments, 10–20 mm), R$_2$ (siltstone fragments, 10–20 mm), and R$_3$ (siltstone fragments, 20–30 mm), were prepared for the tests.

Figure 7 shows the SEM images of the clastic rock and shear-zone samples. It can be seen from the images that the minerals on the surface of samples appear as irregular flaky structures, while the boundaries arrange piece by piece and pores seem inconspicuous. It is observed that the bond among particles of soil sample S$_1$ is relatively tight, while more intergranular pores and fewer particles were observed in the images of soil sample S$_2$. Generally, the mineral pieces of soil samples are relatively looser, and the mineral particles in the siltstone sample are larger than those observed in mudstone sample.

The mineral components of the soil and rock samples obtained via X-ray diffraction (XRD) are presented in Table 3. The results indicate that the two rock samples and soil sample S$_2$ are composed mainly of quartz. The rock sample R$_2$ has a higher mineral content of mixed minerals of illite-montmorillonite, while the sample R$_1$ has similar contents of illite-montmorillonite and chlorite. For shear-zone soil samples, the sample S$_2$ has the highest content of quartz and the lowest content of chlorite. It seems that the total mineral contents of sample S$_1$ are close to that in the sample R$_1$. In addition, it is notable that in sample S$_1$ the content of illite-montmorillonite is approximately the same as that of quartz.

It is well-known that quartz, feldspar, and calcite represent detrital minerals while illite, montmorillonite, and chlorite

represent clay minerals. For the detrital minerals, the main component is quartz (SiO$_2$), which forms as particles and exhibits very stable physical and chemical properties. However, the clay minerals, such as illite and chlorite, are very brittle and generally have high hygroscopicity. These properties largely affect the weathering, disintegration, and mechanical properties of materials composed of clay minerals (Terzaghi et al. 1996; Dhakal et al. 2002). In general, the siltstone sample has the largest proportion of clay minerals among all the samples. Although the two soil samples have more detrital minerals than clay minerals, the soil in muddy interlayer has a higher clay content.

Test procedure

Two types of tests were performed: wetting-drying cycles and soaking tests. The purpose of wetting-drying cycles test is to obtain the influence of water on the physical and mechanical properties of shear-zone materials under alternate wet and dry conditions, while the soaking test aims to investigate the effect of chemical solutions and soaking time on the shear-zone soil samples and clastic rock samples.

(1) Wetting-drying cycles test: A cycle of wetting-drying consisted of one wetting and one drying process. The wetting state of the sample was achieved by soaking in distilled water for 24 h; the sample was then dried at a temperature of 40 °C for 24 h. The details of the wetting-drying tests can be found in the literature (Guney et al. 2007; Kalkan 2011; Zhou et al. 2017). In total, 15 wetting-drying cycles were performed in this test.

(2) Soaking test: Three different solutions, namely, HCl reagent, NaOH reagent, and distilled water, which represented acidic, alkaline, and neutral conditions (at pH 2, 14, and 7, respectively) were used for the soaking test. Clastic rock samples underwent these three solutions, while the shear-zone soil samples were only soaked in acidic solutions with pH 2, which can accelerate the process of interaction between water and soil (Utomo and Dexter 1981; Gratchev and Towhata 2013). Subsequently, all the samples were sealed for 45 days. The pH values remained constant during the entire soaking process by adding reagents.

To evaluate the degree of interaction between water and shear-zone samples, a series of relevant tests, namely, reversal
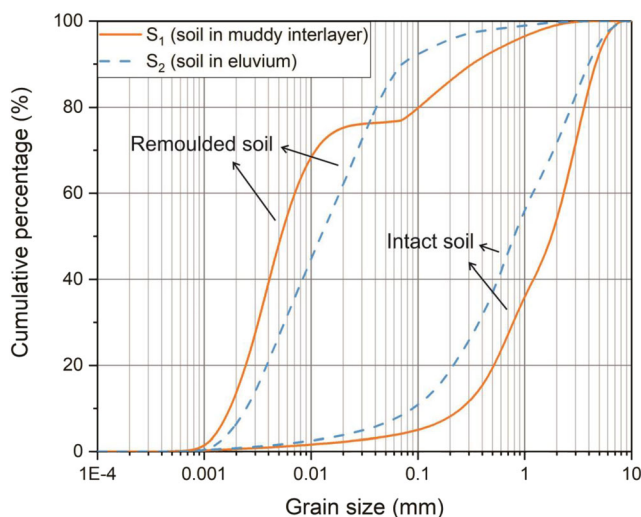
Fig. 4 Grain size distribution of soil samples

Fig. 5 Laser testing results of soil samples. **a** Fine-grained size distribution ($d < 0.1$ mm); **b** frequency distribution of the finer grain ($d < 0.1$ mm)
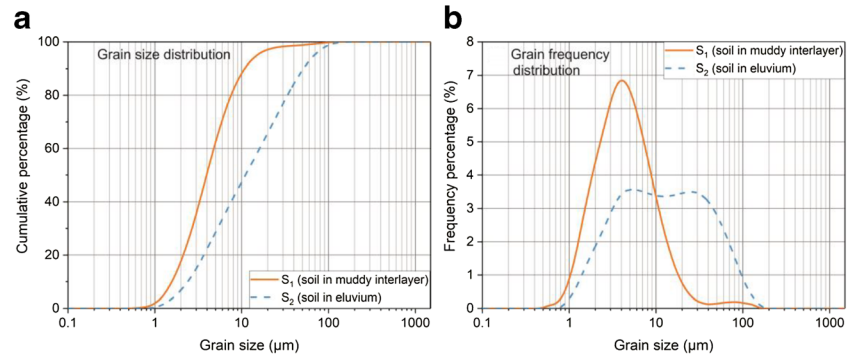
direct shear tests for shear-zone soil samples and grain size distribution for clastic rock samples, were carried out. For the reversal direct shear test, some shear-zone soil samples were reserved after fluid-solid interaction. These samples were then sheared using conventional direct shear apparatus at a rate of 0.02 mm/min under different effective normal stresses (100, 200, 300, and 400 kPa). The first shearing of the reversal direct shear test is the same as that of the conventional direct shear test. At the end of each shearing, the shear box was pulled back to the start point at a rate of 0.5 mm/min. Prior to each reversal shearing, the sample was consolidated for 30 min. Normally, six repeated shearing with 48 mm shear displacement were required to achieve the residual state. On the other hand, for the clastic rock samples, grain size analysis was performed at certain soaking time and wetting-drying cycles. The test was carried out with dried rock samples using the sieving method. Additionally, the mineral composition change of the tested samples was measured by XRD analysis, using particles below 0.075 mm in diameter. Details on the procedures of all the involved tests are provided in Table 4.

Test results

Behaviour of the clastic rock samples

During the wetting-drying cycles and soaking tests, cracks and bubbles were observed on the surface of the rock samples after

24 h. The solution with the mudstone sample became turbid earlier than that with the siltstone sample. Moreover, the mudstone sample became fragmented faster than the siltstone sample. The disintegration behaviour of two clastic rock samples after testing is shown in Fig. 8.

Particle disintegration characteristics Figure 9 shows the changes in the particles after the wetting-drying cycle tests. During the wetting-drying test, the changes in the proportion of large particles ($d > 10$ mm) predominately occurred in the first 3 cycles. The sample R_1 (mudstone) has the fastest and largest reduction in large particles, while sample R_2 (siltstone) changed relatively little and, only decreases by 25.7% after 15 cycles. For sample R_1 (mudstone), the increase in coarse-grained particles with a diameter ranging from 2 to 10 mm is much larger than that of the other samples. In particular, the particles with diameter ranging from 5 to 10 mm increased significantly in the early stage, whereas those ranging from 2 to 5 mm increase mainly in the later stage. In contrast, the sample R_3 (siltstone) accounted for the minimum increase in this range. Fine-grained particles ($d < 2$ mm) produced by sample R_1 grows quickly in the early stage. After nine wetting-drying cycles, the proportion of fine-grained particles produced by samples R_2 and R_3 (siltstone) are identical and exceeds that of the sample R_1.

The wetting-drying cycles disintegrated the mudstone sample to coarse-grained particles with diameters ranging from 2 to 10 mm. In contrast, the siltstone samples were mainly

Fig. 6 Slice images of bedrock samples. **a** Muddy sandstone. **b** Silty mudstone
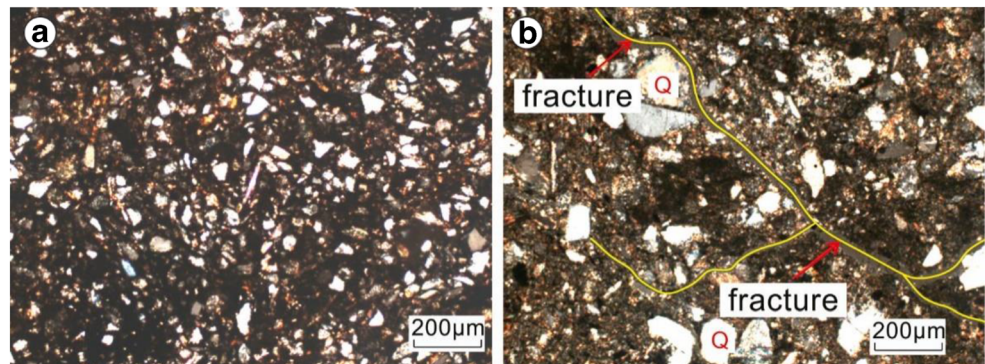
Fig. 7 SEM images of the shear-zone samples. **a** Fractured surface of rock sample R_1; **b** fractured surface of rock sample R_2; **c** soil sample S_1; **d** soil sample S_2
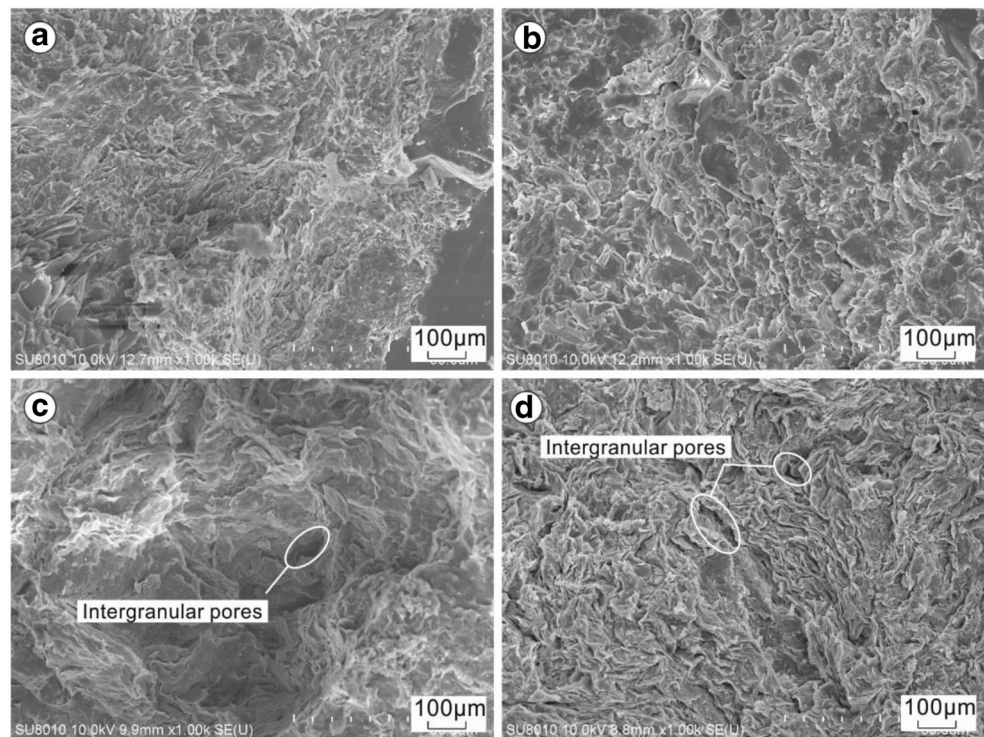
disintegrated to fine-grained particle with diameter less than 2 mm. Similarly, the sample R_3 with an original diameter ranging from 20 to 30 mm also produced a significant fraction of fine-grained particles.

The grain size distributions of the rock sample during soaking test at different pHs are shown in Fig. 10, the sample R_1 (mudstone) experienced dramatic growth in particles larger than 2 mm with alkaline environment, while fine-grained particles (< 2 mm) are more likely to be produced in the acidic environment, and eventually, the fraction of fine-grained particles reached a content of 0.79 wt.%. Compared to the mudstone sample, the siltstone samples soaked in different solutions underwent a much slower disintegration rate for the same soaking time. Among the three solutions, the siltstone sample produced the largest fraction of fine-grained particles in neutral solution at pH 7.

Next, we compare the results of wetting-drying cycles and soaking tests in neutral solution. Generally, the wetting-drying cycles lead to faster disintegration rates than the soaking test.

For example, after the first three cycles, samples R_1 and R_2 produce more large particles ($d > 10$ mm) than that produced by the 45-day soaking. Although the disintegration rate of siltstone is not competitive with that of the mudstone at the beginning, the fraction of fine-grained particles ($d < 2$ mm) exceeds that produced by mudstone after nine wetting-drying cycles. However, this phenomenon is not observed in the soaking tests.

Mineral change characteristics Table 5 shows the changes in mineral composition of rock samples after the tests. An inspection of the results suggests that clay minerals increased in all scenarios, with the soaking test in neutral condition accounting for the smallest increment. Under the acidic conditions, i.e. at pH 2, some detrital minerals, such as quartz, calcite, and feldspar, may be dissolved and converted to clay mineral (Fogler et al. 1975; Huang et al. 1986; Franklin et al. 1994). This situation is, however, unlikely to occur under strong alkaline condition.

Table 3 Mineral proportions of shear-zone samples (%)

| Samples	Chlorite	Illite/montmorillonite	Quartz	Feldspar	Calcite
R_1 (mudstone)	25.5	21.3	35.6	16.8	0.8
R_2 (siltstone)	6.6	31.9	43.5	16.5	1.6
S_1 (soil in muddy interlayer)	8.8	38.9	38.8	13.5	–
S_2 (soil in eluvium)	3.8	17.1	54.3	24.8	–

Table 4 Test procedures on shear-zone materials

Sample name	Description		Test method and conditions		Supplementary analysis	
			Wetting-drying cycles	Soaking test		
R_1	Clastic rock	Mudstone fragment, 10–20 mm	15 cycles at pH 7	At pH 2, 7, 14 for 45 days	Grain size distribution	X-ray diffraction
R_2		Siltstone fragment, 10–20 mm				
R_3		Siltstone fragment, 20–30 mm				
S_1	Shear-zone soil	Main shear-zone in muddy interlayer		At pH 2 for 45 days	Reversal direct shear test	
S_2		Secondary shear-zone in eluvium				

Behaviour of the shear-zone soil samples

Strength-weakening characteristics Figure 11 shows shear strength envelopes of the soil samples under different effective normal stresses. In both the wetting-drying cycles and soaking tests, a reduction in shear strength is observed. For the sample S_1, soil in the muddy interlayer, the soaking test has a more dramatic influence on the peak strength, while the residual strength exhibits a more sensitive response to the wetting-drying cycle test. With a larger effective normal stress, the decrease of residual strength is more evident after 15 wetting-drying cycles. The wetting-drying cycles and soaking tests give rise to a similar reduction tendency in shear strength of the soil samples S_1 and S_2, whereas soaking leads to a larger reduction in the residual strength.

For both testing conditions, the decrease in peak strength of soil samples is much greater than the residual strength, which indicates that the fluid-solid interaction may cause a distinct reduction in peak strength. The situation is likely to occur when a landslide is under extreme hydraulic conditions and subsequently causes a sudden motion. It was also observed that the sample S_2 achieved a residual state earlier than the S_1 sample, and a higher residual strength was obtained, indicating the clay particles in sample S_2 are oriented faster during shearing (Skempton 1985). Note that the residual strength of the sample S_1 decreased more after 15 wetting-drying cycles, while sample S_2 is more affected by soaking. This phenomenon helps to explain why the shear-zone soil in the muddy interlayer is more fragile and easily disturbed in natural conditions, especially when encountered wet-dry alternations, which accounts for a crucial factor of landslides.
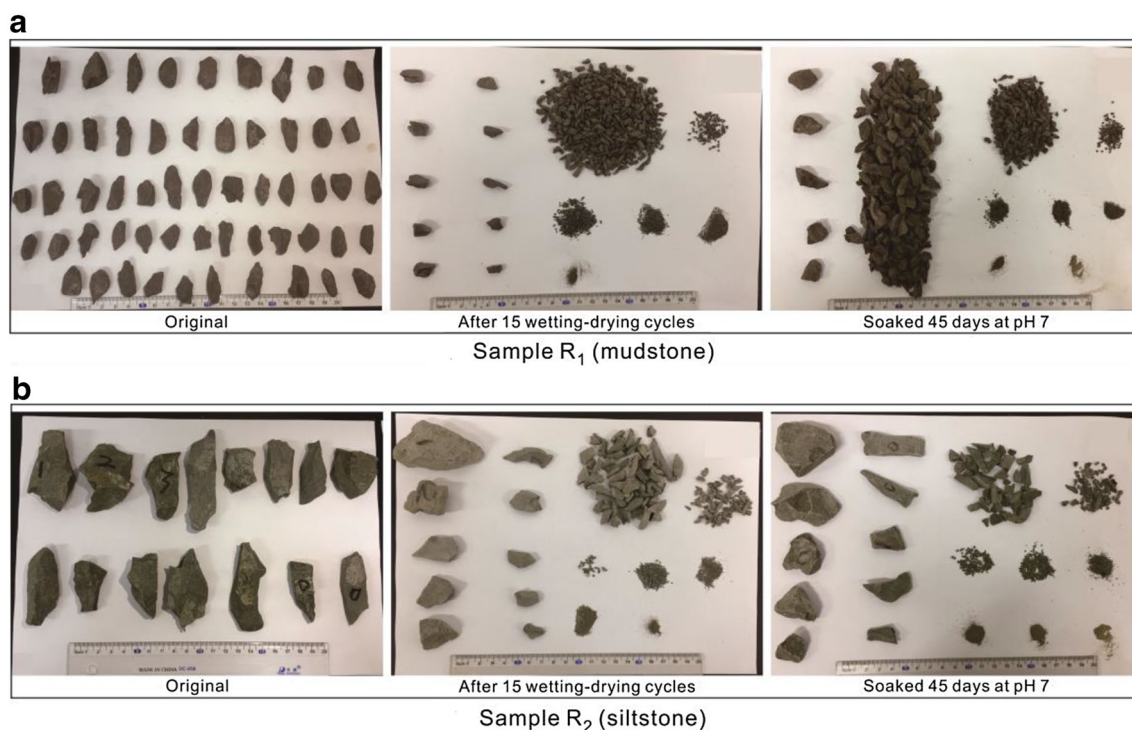
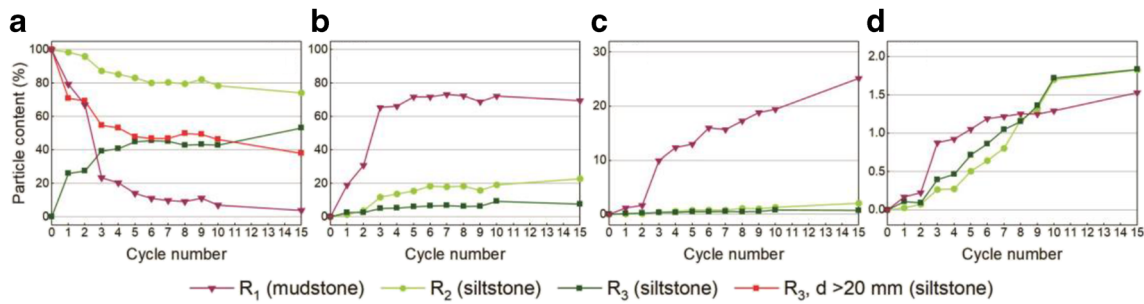**Fig. 8** Disintegration of mudstone and siltstone samples

Fig. 9 Grain size distribution of rock samples during the wetting-drying test. **a** $d < 10$ mm; **b** $5 < d < 10$ mm; **c** $2 < d < 5$ mm; and **d** $d < 2$ mm

Variations in the friction angle and cohesion of the soil samples are shown in Fig. 12. Generally, the cohesion and friction angle decrease as the wetting-drying cycles and soaking time increase. During the wetting-drying cycle tests, the cohesion of sample S_1 decreases mostly from the 3rd to the 5th cycles while the friction angle predominately decreases in the first 3 cycles. For sample S_2, the peak cohesion decreases in the first 6 cycles until an asymptotic residual state is reached. Both the peak and residual friction angle exhibit a gradual decrease, and an approximately 20% reduction is observed at the end of the wetting-drying cycle test.

In the soaking condition, the sample S_1 shows a sudden reduction in cohesion and friction angle at the onset of soaking. As the soaking time increased, the cohesion continues to decrease, while the friction angle reaches a steady state. It is interesting to note that a similar reduction, approximately 20%, in both residual and peak friction angles is observed after 45-day soaking. For sample S_2, the cohesion
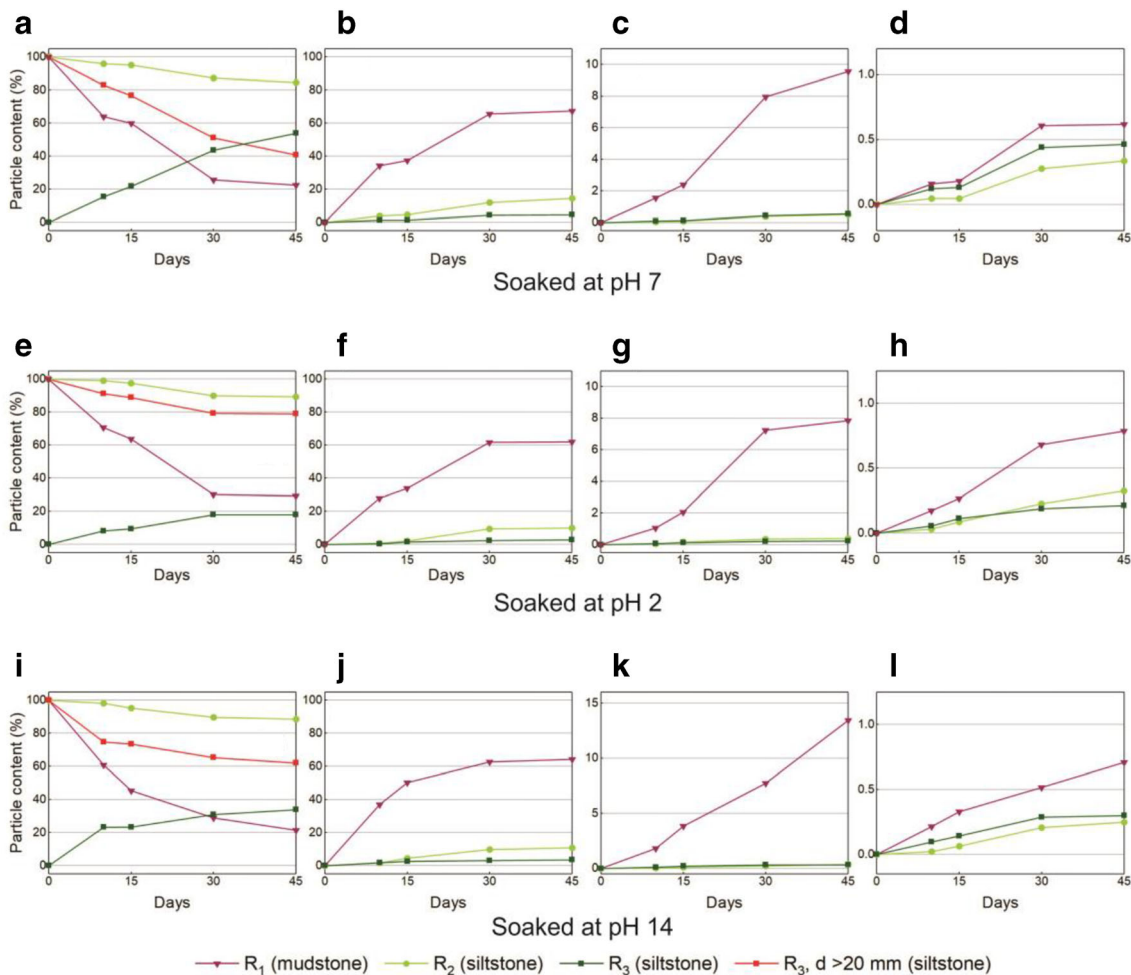

Fig. 10 Grain size distribution of rock samples during the soaking test. **a, e, i**, $d > 10$ mm; **b, f, g** $5 < d < 10$ mm; **c, g, k** $2 < d < 5$ mm; and **d, h, l** $d < 2$ mm

**Table 5** Mineral composition results of rock samples by XRD (%)

Samples	Test conditions	Chlorite	Illite/montmorillonite	Quartz	Feldspar	Calcite	Clay mineral	Detrital mineral
R_1 (mudstone)	Original	25.5	21.3	35.6	16.8	0.8	46.8	53.2
	After 15 wetting-drying cycles	23.9	27.1	27.7	18.6	2.7	51.0	49.0
	Soaked for 45 days at pH 7	24.7	24.0	33.6	16.0	1.8	48.7	51.3
	Soaked for 45 days at pH 2	24.7	29.1	36.0	10.2	0.0	53.8	46.3
	Soaked for 45 days at pH 14	25.4	25.5	32.1	16.9	2.1	50.9	49.1
R_2 (siltstone)	Original	6.6	31.9	43.5	16.5	1.6	38.5	61.5
	After 15 wetting-drying cycles	11.0	28.9	37.6	20.4	2.2	39.9	60.1
	Soaked for 45 days at pH 7	8.5	30.4	42.5	16.1	2.5	38.9	61.1
	Soaked for 45 days at pH 2	10.3	34.3	40.8	14.6	0.0	44.6	55.4
	Soaked for 45 days at pH 14	8.3	32.9	39.0	17.8	2.0	41.2	58.8

decreases continuously from approximately 11 kPa at the beginning to 1.1 kPa at the end of the soaking test, while the residual friction angle experiences a much higher decrease. The test results reveal that the effects of fluid-solid interaction are more significant for the friction angle of sample S_1 taken from the muddy interlayer, while the cohesion of sample S_2 taken from eluvium is more sensitive for the interaction.

Mineral changes characteristics Table 6 shows the mineral composition of soil samples during the tests. The proportions of the detrital mineral gradually decrease, while the clay minerals increase at the same time. This phenomenon indicates that detrital mineral may have been partially converted to clay mineral during the interaction. The proportion of clay minerals in sample S_1 increases fastest during the 3rd to 5th cycles in the wetting-drying cycles test. The content of clay minerals becomes 1.2% larger than that of the detrital minerals after 15 cycles. This conversion process is significantly accelerated by soaking since the content of clay minerals already exceeds that of the detrital minerals after 5-day soaking, and a high content of 58.6% is achieved in the end.

Fig. 11 Shear strength envelope of soil samples by reversal shear tests in peak and residual states. **a, b** sample S_1 (soil in muddy interlayer); **c, d** sample S_2 (soil in eluvium)
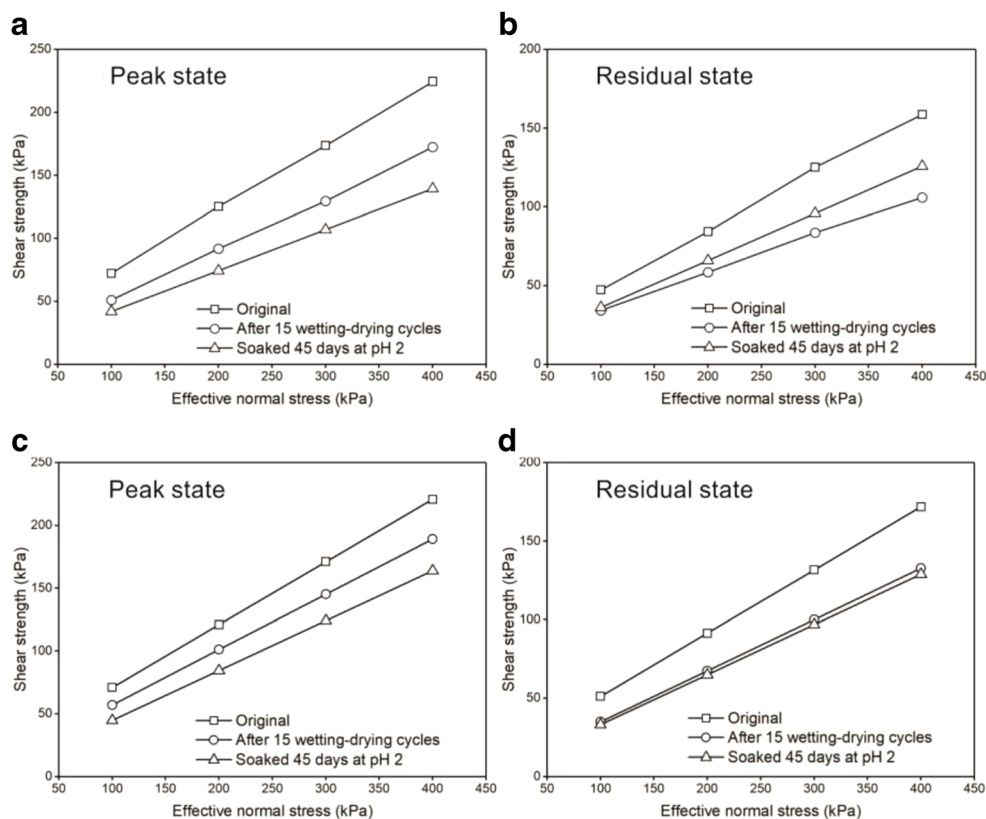
Fig. 12 Cohesion and friction angle of the soil samples during the test in peak and residual states. **a**, **b** wetting-drying test; **c**, **d** soaking test
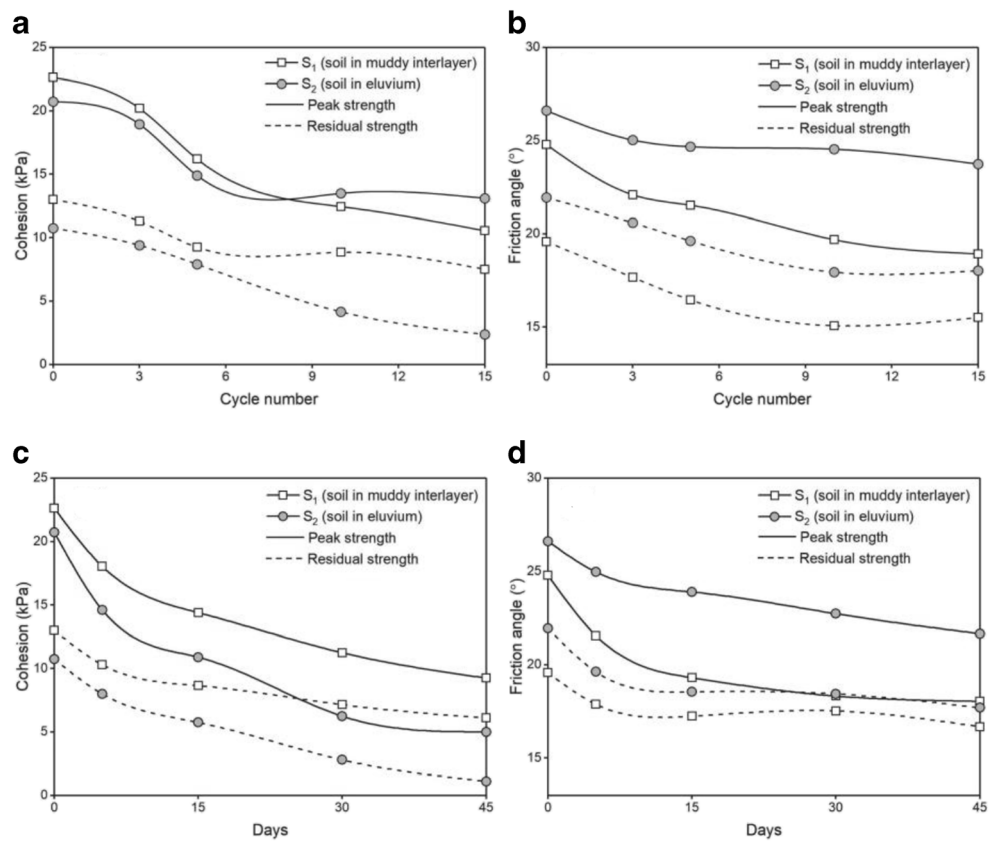
Compared to sample S_1, however, the clay minerals of sample S_2 grow much more slowly and does not exceed the content of detrital minerals at the end of the test. Obviously, the soaking test gives rise to faster growth of the clay minerals, and the clay minerals of the soil samples in the muddy interlayer are more sensitive to fluid-solid interaction. Correspondingly, both wetting-drying cycles and long-term soaking will accelerate the conversion of detrital minerals to clay minerals in the soil from shear zones and subsequently increase of the potential for argillization.

Discussions

Minerals conversion at different pHs

Argillization is known to account for an important step that generates shear-zone soil (Gibo et al. 1987; Tang et al. 2015). In our case, we specialized to investigate the mineral content of the tested samples against time because the clay content in fine-grained particles reflects the ability of argillization in shear-zone materials. Therefore, it is important to understand how the detrital minerals convert to clay mineral during the fluid-solid interaction with chemical solutions.

Table 7 shows the reaction equations of mineral dissolution in different acid-base environments. For detrital minerals in the shear-zone soil samples and clastic rock samples, calcite dissolves rapidly and K^+ and Na^+ in feldspar will be replaced by H^+ in acidic solution (Raeside 1959). This reaction leads to the formation of the colloidal precipitate (H_4SiO_4), which provides material for the generation of clay minerals. In the alkaline solution, quartz is more likely to convert into phyllosilicate (H_2SiO_2), which may be related to the generation of the flocculent montmorillonite (Lim and Jackson 1986; Reinholdt et al. 2005).

The test results show that both mudstone and siltstone samples experienced pronounce reductions in feldspar content, while the proportion of montmorillonite-illite minerals and chlorite increase in the mudstone and siltstones samples, respectively. Feldspar and quartz in the two soil samples decrease dramatically, which proves that they are the main source of the increase of the clay minerals. This phenomenon is, however, hardly observed in nature because the chemical interaction is very slow in the natural state, while the acidic environment in the test accelerates the process.

As the most common clay minerals in mudstone stratum, the mixed minerals of illite, montmorillonite, and chlorite characterize the mechanical properties of rock and soil (Taylor and Smith 1986; Siegesmund et al. 2018). According to the above analysis, the shear-zone materials of the Shanshucao landslide will continuously convert to clay minerals, which irreversibly leads to the generation of shear

Table 6 Mineral composition results of the soil samples by XRD (%)

Samples	Test conditions		Chlorite	Illite/montmorillonite	Quartz	Feldspar	Clay mineral	Detrital mineral
S_1 (soil in muddy interlayer)	Original		8.8	38.9	38.8	13.5	47.7	52.3
	Wetting-drying cycles	3 cycles	9.4	38.0	40.7	12.0	47.4	52.6
		5 cycles	10.6	37.7	42.8	8.9	48.3	51.7
		10 cycles	8.5	40.2	41.3	10.0	48.7	51.3
		15 cycles	10.0	40.6	42.6	6.8	50.6	49.4
	Soaking at pH 2	5 days	9.3	43.8	36.8	10.1	53.2	46.9
		15 days	10.4	46.6	35.5	7.5	57.0	43.1
		30 days	12.3	45.8	36.1	5.7	58.2	41.8
		45 days	13.3	45.3	37.6	3.8	58.6	41.4
S_2 (soil in eluvium)	Original		3.8	17.1	54.3	24.8	20.9	79.1
	Wetting-drying cycles	3 cycles	4.4	17.2	55.4	23.0	21.6	78.4
		5 cycles	4.4	16.2	59.0	20.4	20.6	79.4
		10 cycles	9.4	12.3	56.5	21.8	21.7	78.3
		15 cycles	9.9	12.7	55.2	22.2	22.6	77.4
	Soaking at pH 2	5 days	7.0	15.3	57.6	20.1	22.3	77.8
		15 days	8.0	15.3	58.8	17.8	23.4	76.6
		30 days	11.5	13.3	57.3	17.9	24.8	75.2
		45 days	11.7	13.7	55.9	18.7	25.4	74.6

zone regardless of the process, i.e. wetting-drying cycles and soaking conditions.

Evolutionary relationship of shear-zone materials

To gain a deeper insight into the effects of fluid-solid interaction on the shear strength-weakening behaviour, Fig. 13a compares the fraction of fine-graded particles in the intact soil samples (S_1 and S_2) and in the clastic rock (R_1 and R_2) after soaking for 45 days in the neutral solution. Additionally, a weathering product of quartz sandstone from the landslide area was tested for comparison. The comparison shows that more fine-grained particles were produced by the sample S_1. As shown in Fig. 13b, all the soaked rock samples and the weathering product exhibit similar grain size distribution as

that measured from the sample S_2 (soil in eluvium), while a plateau characterized by particles with a size of approximately 30 μm is observed in the three samples. The analysis indicates that the soil sample S_2 is more likely to originate from the silty mudstone, argillaceous siltstone, and quartz sandstone in the shear zones of the landslide.

It is worth noting that there still exhibits debate in the origin and evolution of the shear-zone soil in the muddy interlayer. The shear-zone materials of the landslide are distributed in a wide range and usually exhibit nonuniform characteristics. However, the samples used in our tests cannot represent all the characteristics. Moreover, in real situations, the interaction between water and slope materials occurs over a long period, while this process is hard to replicate in the laboratory due to the limitation of test time.

Table 7 Reaction equation of mineral dissolution (Feng et al. 2010)

Minerals	Reaction equation	Solutions
Quartz	$SiO_2 + 2H_2O = H_4SiO_4$	Neutral and acidic
	$SiO_2 + 2OH^- = H_2SiO_2^-$	Alkaline
Calcite	$CaCO_3 = Ca^{2+} + CO_3^{2-}$	Neutral and alkaline
	$CaCO_3 + 2H^+ = Ca^{2+} + H_2O + CO_2$	Acidic
Albite	$NaAlSi_3O_8 + 5.5H_2O = 0.5Al_2Si_2O_5(OH)_4 + Na^+ + OH^- + 2H_4SiO_4$	Neutral
	$NaAlSi_3O_8 + 4H^+ + 4H_2O = Na^+ + Al^{3+} + 3H_4SiO_4$	Acidic
	$NaAlSi_3O_8 + 6OH^- + 2H_2O = Na^+ + Al(OH)_4^- + 3H_2SiO_4^{2-}$	Alkaline
Potash feldspar	$KAl_2Si_3O_8 + 5.5H_2O = 0.5Al_2Si_2O_5(OH)_4 + K^+ + OH^- + 2H_4SiO_4$	Neutral
	$KAlSi_3O_8 + 4H^+ + 4H_2O = K^+ + Al^{3+} + 3H_4SiO_4$	Acidic
	$KAlSi_3O_8 + 6OH^- + 2H_2O = K^+ + Al(OH)_4^- + 3H_2SiO_4^{2-}$	Alkaline

Fig. 13 Fine-grained distribution obtained by laser testing after tests ($d < 0.01$ mm). **a** Grain size distribution of different samples. **b** Grain frequency distribution of different samples
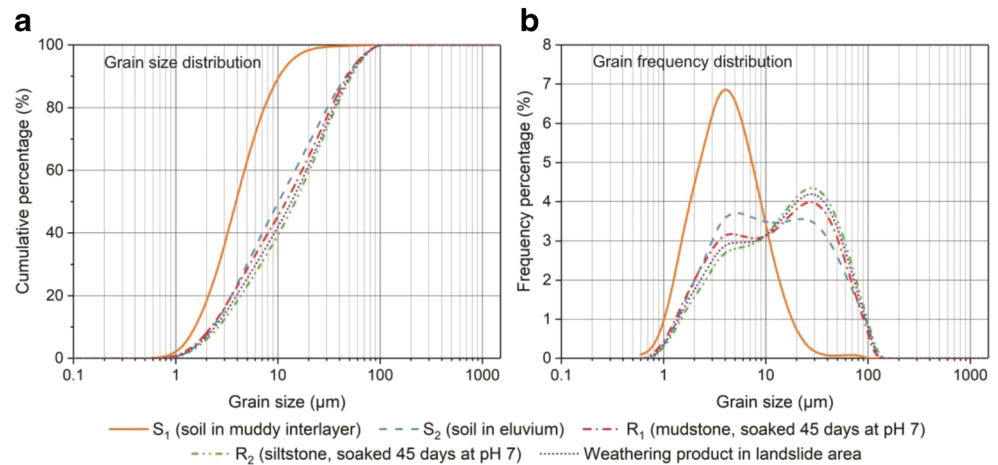
Conclusions

This paper investigates the interaction between water and shear-zone materials taken from a bedding landslide in the TGR area of China. A series of wetting-drying cycles and soaking (at different pHs) tests are carried out on both shear-zone soil and clastic rock. The intensity of the interaction is characterized by some widely used soil indexes, such as shear strength and grain size distribution. The following conclusions can be drawn:

(1) The shear strength of the shear-zone soil in the muddy interlayer is lower than that in the eluvium, while a longer shear displacement is required by the former to achieve the residual state. Compared to the wetting-drying cycles, the effect of soaking on the reduction in shear strength of the shear-zone soil is more significant. The fluid-solid interaction results in a greater fraction of clay minerals for the shear-zone soil from the muddy interlayer.

(2) The weakening effect of water on clastic rocks from the shear zone appears as a dramatic promotion of disintegration. After 15 wetting-drying cycles, the siltstone sample produces the most significant fine-grained particles. In addition, soaking in acidic and alkaline solutions can accelerate the process of fine-grained production, and the acidic environment can significantly increase the clay mineral content of all the clastic rock samples.

In summary, the fluid-solid interaction is able to affect the shear strength of the shear-zone soils and the disintegration rate of the clastic rocks in the shear zones. Furthermore, this interaction can promote the production of the clay minerals in the shear-zone soil, which may relate to the formation of shear zones; therefore, we speculate that the clastic rocks in the shear zones may be the parent materials of the shear-zone soils. The experimental results suggest that the effects of wetting-drying cycles and soaking play a significant role in the evolution of the shear zone in the TGR area.

References

Aldaood A, Bouasker M, Al-Mukhtar M (2014) Impact of wetting–drying cycles on the microstructure and mechanical properties of lime-stabilized gypseous soils. Eng Geol 174:11–21. https://doi.org/10.1016/j.enggeo.2014.03.002

Baum RL, Godt JW, Savage WZ (2010) Estimating the timing and location of shallow rainfall-induced landslides using a model for transient, unsaturated infiltration. Journal of Geophysical Research: Earth Surface 115(F3). https://doi.org/10.1029/2009JF001321

Bjerrum L, Rosenqvist IT (1956) Some experiments with artificially sedimented clays. Géotechnique 6(3):124–136. https://doi.org/10.1680/geot.1956.6.3.124

Calvello M, Lasco MK, Vassallo R, Di Maio C (2005) Compressibility and residual shear strength of smectitic clays: influence of pore aqueous solutions and organic solvents. Italian Geotechnical Journal 1(2005):34–46

Dhakal G, Yoneda T, Kato M, Kaneko K (2002) Slake durability and mineralogical properties of some pyroclastic and sedimentary rocks. Eng Geol 65(1):31–45. https://doi.org/10.1016/S0013-7952(01)00101-6

Di Maio C, Santoli L, Schiavone P (2004) Volume change behaviour of clays: the influence of mineral composition, pore fluid composition and stress state. Mech Mater 36(5–6):435–451. https://doi.org/10.1016/S0167-6636(03)00070-X

Di Maio C, Scaringi G, Vassallo R (2015) Residual strength and creep behaviour on the slip surface of specimens of a landslide in marine origin clay shales: influence of pore fluid composition. Landslides 12(4):657–667. https://doi.org/10.1007/s10346-016-0737-z

Dif AE, Bluemel WF (1991) Expansive soils under cyclic drying and wetting. Geotech Test J 14(1):96–102. https://doi.org/10.1520/GTJ10196J

Feng XT, Ding WX, Yao HY, Cui Q, Chen SL (2010) Coupled chemical-stress effect on rock fracturing process. Science Press, Beijing

Fogler HS, Lund K, McCune CC (1975) Acidization III—the kinetics of the dissolution of sodium and potassium feldspar in HF/HCl acid mixtures. Chem Eng Sci 30(11):1325–1332. https://doi.org/10.1016/0009-2509(75)85061-5

Franklin SP, Hajash JA, Dewers TA, Tieh TT (1994) The role of carboxylic acids in albite and quartz dissolution: an experimental study

under diagenetic conditions. Geochim Cosmochim Acta 58(20): 4259–4279. https://doi.org/10.1016/0016-7037(94)90332-8

Gibo S, Egashira K, Ohtsubo M (1987) Residual strength of smectite-dominated soils from the Kamenose landslide in Japan. Can Geotech J 24(3):456–462. https://doi.org/10.1139/t87-057

Gratchev I, Towhata I (2013) Stress-strain characteristics of two natural soils subjected to long-term acidic contamination. Soils Found 53(3):469–476. https://doi.org/10.1016/j.sandf.2013.04.008

Guney Y, Sari D, Cetin M, Tuncan M (2007) Impact of cyclic wetting–drying on swelling behavior of lime-stabilized soil. Build Environ 42(2):681–688. https://doi.org/10.1016/j.buildenv.2005.10.035

Huang WL, Bishop AM, Brown RW (1986) The effect of fluid/rock ratio on feldspar dissolution and illite formation under reservoir conditions. Clay Miner 21(4):585–601. https://doi.org/10.1180/claymin.1986.021.4.10

Iverson RM (2000) Landslide triggering by rain infiltration. Water Resour Res 36(7):1897–1910. https://doi.org/10.1029/2000WR900090

Kalkan E (2011) Impact of wetting–drying cycles on swelling behavior of clayey soils modified by silica fume. Appl Clay Sci 52(4):345–352. https://doi.org/10.1016/j.clay.2011.03.014

Kanyaya JI, Trenhaile AS (2005) Tidal wetting and drying on shore platforms: an experimental assessment. Geomorphology 70(1–2): 129–146. https://doi.org/10.1016/j.geomorph.2005.04.005

Lim CH, Jackson ML (1986) Expandable phyllosilicate reactions with lithium on heating. Clay Clay Miner 34(3):346–352. https://doi.org/10.1346/CCMN.1986.0340316

Lora M, Camporese M, Troch PA, Salandin P (2016) Rainfall-triggered shallow landslides: infiltration dynamics in a physical hillslope model. Hydrol Process 30(18):3239–3251. https://doi.org/10.1002/hyp.10829

Majdalani S, Michel E, Di-Pietro L, Angulo-Jaramillo R (2008) Effects of wetting and drying cycles on in situ soil particle mobilization. Eur J Soil Sci 59(2):147–155. https://doi.org/10.1111/j.1365-2389.2007.00964.x

McKissock I, Gilkes RJ, Walker EL (2002) The reduction of water repellency by added clay is influenced by clay and soil properties. Appl Clay Sci 20(4–5):225–241. https://doi.org/10.1016/S0169-1317(01)00074-6

Mesri G, Olson RE (1970) Shear strength of montmorillonite. Géotechnique 20(3):261–270. https://doi.org/10.1680/geot.1970.20.3.261

Müller B, Berg M, Yao ZP, Zhang XF, Wang D, Pfluger A (2008) How polluted is the Yangtze river? Water quality downstream from the Three Gorges Dam. Sci Total Environ 402(2–3):232–247. https://doi.org/10.1016/j.scitotenv.2008.04.049

Özbek A (2014) Investigation of the effects of wetting–drying and freezing–thawing cycles on some physical and mechanical properties of selected ignimbrites. Bull Eng Geol Environ 73(2):595–609. https://doi.org/10.1007/s10064-013-0519-y

Paronuzzi P, Rigo E, Bolla A (2013) Influence of filling–drawdown cycles of the Vajont reservoir on Mt. Toc slope stability. Geomorphology 191:75–93. https://doi.org/10.1016/j.geomorph.2013.03.004

Raeside JD (1959) Stability of index minerals in soils with particular reference to quartz, zircon, and garnet. J Sediment Res 29(4):493–502. https://doi.org/10.1306/74D7097F-2B21-11D7-8648000102C1865D

Reinholdt M, Miehe-Brendle J, Delmotte L, Le Dred R (2005) Synthesis and characterization of montmorillonite-type phyllosilicates in a fluoride medium. Clay Miner 40(2):177–190. https://doi.org/10.1180/0009855054020164

Siegesmund S, Sousa L, Knell C (2018) Thermal expansion of granitoids. Environ Earth Sci 77(2):41. https://doi.org/10.1007/s12665-017-7119-2

Skempton AW (1985) Residual strength of clays in landslides, folded strata and the laboratory. Géotechnique 35(1):3–18. https://doi.org/10.1680/geot.1985.35.1.3

Sridharan A, Prakash K (1999) Influence of clay mineralogy and pore-medium chemistry on clay sediment formation. Can Geotech J 36(5):961–966. https://doi.org/10.1139/t99-045

Tang CS, Cui YJ, Shi B, Tang AM, Liu C (2011) Desiccation and cracking behaviour of clay layer from slurry state under wetting–drying cycles. Geoderma 166(1):111–118. https://doi.org/10.1016/j.geoderma.2011.07.018

Tang H, Li C, Hu X, Su A, Wang L, Wu Y, ... Li Y (2015) Evolution characteristics of the Huangtupo landslide based on in situ tunneling and monitoring. Landslides, 12(3):511–521. DOI: https://doi.org/10.1007/s10346-014-0500-2

Taylor RK, Smith TJ (1986) The engineering geology of clay minerals: swelling, shrinking and mudrock breakdown. Clay Miner 21(3): 235–260. https://doi.org/10.1180/claymin.1986.021.3.01

Terzaghi K, Peck RB, Mesri G (1996) Soil mechanics. John Wiley & Sons, New York

Utomo WH, Dexter AR (1981) Soil friability. J Soil Sci 32(2):203–213. https://doi.org/10.1111/j.1365-2389.1981.tb01700.x

Wang FW, Zhang YM, Huo ZT, Matsumoto T, Huang BL (2004) The July 14, 2003 Qianjiangping landslide, Three Gorges Reservoir, China. Landslides 1(2):157–162. https://doi.org/10.1007/s10346-004-0020-6

Wang S, Wu W, Wang JE, Yin ZY, Cui DS, Xiang W (2018) Residual-state creep of clastic soil in a reactivated slow-moving landslide in the Three Gorges Reservoir Region, China. Landslides 15(12): 2413–2422. https://doi.org/10.1007/s10346-018-1043-8

Wang S, Wang JE, Wu W, Cui DS, Su AJ, Xiang W (2020) Creep properties of clastic soil in a reactivated slow-moving landslide in the Three Gorges Reservoir Region, China. Eng Geol 267:105493. https://doi.org/10.1016/j.enggeo.2020.105493

Xia M, Ren GM, Zhu SS, Ma XL (2015) Relationship between landslide stability and reservoir water level variation. Bull Eng Geol Environ 74(3):909–917. https://doi.org/10.1007/s10064-014-0654-0

Xu G, Li W, Yu Z, Ma X, Yu Z (2015) The 2 September 2014 Shanshucao landslide, Three Gorges Reservoir, China. Landslides 12(6):1169–1178. https://doi.org/10.1007/s10346-015-0652-8

Ye C, Li S, Zhang Y, Zhang Q (2011) Assessing soil heavy metal pollution in the water-level-fluctuation zone of the Three Gorges Reservoir, China. J Hazard Mater 191(1–3):366–372. https://doi.org/10.1016/j.jhazmat.2011.04.090

Zhou Z, Cai X, Chen L, Cao W, Zhao Y, Xiong C (2017) Influence of cyclic wetting and drying on physical and dynamic compressive properties of sandstone. Eng Geol 220:1–12. https://doi.org/10.1016/j.enggeo.2017.01.017